

AN ABSTRACT OF THE THESIS OF

Adam Lambert for the degree of Master of Science in Chemical Engineering
presented on August 16, 2010.

Title:

Advection-diffusion in Inertial Flow through Periodically Converging-diverging Tubes.

Abstract approved: _____

Brian Wood

A direct numerical simulation of advection-diffusion in a sinusoidal tube was carried out using the commercial finite-volume code STAR-CD. The Reynolds numbers varied from $Re = 0.1$ to $Re = 14.5$. At the larger Reynolds numbers, steady-state eddies formed in the diverging sections and significantly influenced the macroscale dispersion. Long tailing was observed in the breakthrough curves. The results were compared to a 1-dimensional source-sink model using the semi-analytical solute transport code STAMMT-L. It was found that the results were generally described by both a single-rate model and a lognormal multi-rate model. It was observed that the velocity distribution within the inertial regime had significant influence on dispersion, even at weak inertial flowrates which did not experience flow separation.

©Copyright by Adam Lambert
August 16, 2010
All Rights Reserved

Advection-diffusion in Inertial Flow through Periodically
Converging-diverging Tubes.

by

Adam Lambert

A THESIS

submitted to

Oregon State University

in partial fulfillment of
the requirements for the
degree of

Master of Science

Presented August 16, 2010
Commencement June 2011

Master of Science thesis of Adam Lambert presented on August 16, 2010.

APPROVED:

Major Professor, representing Chemical Engineering

Head of the School of the Oregon State University of Chemical, Biological, and Environmental Engineering

Dean of the Graduate School

I understand that my thesis will become part of the permanent collection of Oregon State University libraries. My signature below authorizes release of my thesis to any reader upon request.

Adam Lambert, Author

ACKNOWLEDGEMENTS

I would like to thank Dr. Brian Wood, my family, and my beautiful dog Quito.

TABLE OF CONTENTS

	<u>Page</u>
1 Introduction	1
1.1 Motivation	1
1.2 Introduction to the classical problem of mass transport in a capillary tube	1
1.2.1 Momentum Transport	2
1.2.2 Mass Transport: Microscale	3
1.2.3 Mass Transport: Macroscale	3
1.3 The dispersive process studied in this work	5
2 Literature Review	8
2.1 Model Problems: Straight tubes	8
2.2 Taylor Dispersion: Early Time Solutions	10
2.3 Model problems: More complex geometries	12
2.4 Models for dispersion	15
3 Numerical Simulation	17
3.1 Geometry and Discretization	17
3.2 Simulation Conditions	18
3.3 Grid Convergence	20
4 Results	22
4.1 Definitions	22
4.2 Flow observations	22
4.3 Advection-Diffusion Observations: Early time	25
4.4 Advection-Diffusion Observations: Late times	28
5 Analysis	30
5.1 General model for advection-dispersion with mass transfer	30
5.2 Development of the source-sink term, $\Gamma(t)$	32
5.2.1 Closure of $\Gamma(t)$	36
5.2.2 $b(\alpha)$ for a single-rate first order system	37

TABLE OF CONTENTS (Continued)

	<u>Page</u>
5.2.3 $b(\alpha)$ for a lognormal distribution of first-order rate coefficients	38
5.3 STAMMT-L 3.0	38
6 Conclusion	41
Bibliography	42

LIST OF FIGURES

<u>Figure</u>		<u>Page</u>
3.1	A segment of sinusoidal tube	17
4.1	Non-inertial streamlines	23
4.2	Streamlines at $Re = 4.5$	24
4.3	Streamlines at $Re = 8.5$	24
4.4	Inertial streamlines at $Re = 14.5$	25
4.5	BTC for all flowrates plotted against residence time, τ	26
4.6	Concentration field for $Re = 4.5$ after the inertial core has initially cleared the central flow	27
4.7	Local concentration field at $Re = 8$	28
4.8	BTC's for all cases with logarithmic concentration scales	29

Chapter 1 – Introduction

1.1 Motivation

Mass transport in capillaries with varying cross section is a component of many engineering problems. In this case the velocity varies not only as function of the radius, but also periodically with the central axis. These pore-scale variations have a significant influence on the macroscale dispersion. In order to better understand the link between pore-scale phenomenon and the macroscale behavior, simple, yet representative, models can be examined. The conclusions from such an analysis can then be used to develop a more descriptive model for complex mass transport.

1.2 Introduction to the classical problem of mass transport in a capillary tube

In general, it is desirable to predict the macroscale behavior of system over time. However, variations in the velocity field at the microscale can contribute significantly to the macroscale dispersion. The length and time scales associated with the microscale flow are many orders of magnitude smaller than the length and time scales associated with the macroscale flow. While the equations governing the microscale flowfield and related mass transport are well understood, direct

numerical simulation over the full microscale domain is not generally possible. As a result, much of the research is focused on predicting the average velocity of the solute and the change in spatial distribution over time in terms of the physical parameters describing the system [Brenner, 1980]. It is common practice to use model geometries to gain understanding of complex physical processes [Hoagland and Prud'homme, 1985]. For example, by studying dispersion within flow through a straight tube, especially a tube with a large aspect (length to diameter) ratio, the relationship between pore scale velocity gradients and the time-variations of the macroscale dispersion may be examined in a controlled setting.

1.2.1 Momentum Transport

The flow of a steady incompressible fluid through a pore is governed by the steady Navier-Stokes equations.

$$\rho(\mathbf{u} \cdot \nabla)\mathbf{u} + \nabla p = \mu \nabla^2 \mathbf{u} \quad (1.1)$$

$$\nabla \cdot \mathbf{u} = 0 \quad (1.2)$$

where ρ is the fluid density, \mathbf{u} is the velocity vector, μ is the dynamic viscosity, and p is the sum of the hydrodynamic and hydrostatic pressures. Appropriate boundary conditions must be applied to generate a solution. Examining the unidirectional flow that occurs within smooth, straight tubes we can conclude that the

velocity gradient is large for a small cross-section.

1.2.2 Mass Transport: Microscale

The transport of a solute within a fluid is governed by the mass balance

$$\frac{\partial c}{\partial t} = D\nabla^2 c + \nabla \cdot \mathbf{u}c \quad (1.3)$$

Where D is the diffusivity of the solute, \mathbf{u} is the velocity vector, and c is the local concentration of the solute. The entire velocity field must be resolved in order for the local advection diffusion equation to be utilized.

1.2.3 Mass Transport: Macroscale

By assuming a 1-dimensional distribution of solute and taking the average of the local concentration, the following macro-scale advection diffusion equation can be generated [Taylor, 1953]:

$$\frac{\partial C}{\partial t} = D_{eff} \frac{\partial^2 C}{\partial x^2} + U \frac{\partial C}{\partial x} \quad (1.4)$$

Where C is the area-averaged concentration, U is the average velocity, and D_{eff} is the effective dispersion coefficient. There has been a great deal of research on determining D_{eff} under various flow conditions. In order for this averaged equation to accurately represent the one-dimensional spreading of a solute, D_{eff} must

accurately capture the effect that pore-scale velocity gradients have on macroscale dispersion within the media at a given macroscale flowrate.

Sir Geoffrey Taylor generated two analytical solutions for one-dimensional dispersion within a straight tube, one based on advection alone, and one based on the combined effect of advection and diffusion [Taylor, 1953]. The assumption was made that radial diffusion occurs quickly compared to the bulk flow of the fluid, and variance in concentration along the radial coordinate was neglected. It was shown that radial velocity gradients within a tube led to redistribution of a slug of solute, increasing both concentration gradients and the surface area over which diffusion occurs [Taylor, 1953]. Taylor then performed an experiment physically measuring the dispersion of potassium permanganate by colorimetry, and the results matched very well with the analytical solution for combined advection-diffusion [Taylor, 1953]. From the analytical solution, Taylor predicted that the dispersion coefficient should be

$$D_{eff} = a^2 U^2 / 192 D_m \quad (1.5)$$

where a is the radius of the tube, U the average velocity, and D_m the molecular diffusivity. Taylor went on to validate the above solution for the following conditions [Taylor, 1954].

$$6.9 \ll aU/D_m \ll 4L/a \quad (1.6)$$

The middle term in the inequality, aU/D_m , is called the Péclet number. It is the non-dimensional ratio of advection rate to diffusion rate. L/a is the aspect

ratio of the tube. In this case, the macroscale behavior is related to the microscale diameter and diffusivity.

Rutherford Aris subsequently published an analytical solution to the advection-diffusion equation for a tube using the method of moments [Aris, 1959b]. His work resulted in the inclusion of the pure molecular diffusion coefficient in the definition of the dispersion coefficient, which was presented as

$$D_{eff} = D_m + a^2 U^2 / 192 D_m \quad (1.7)$$

This definition eliminates Taylor’s lower constraint, which insured that the Péclet number was large enough to overshadow the effect of molecular diffusion, so that only the “apparent diffusion coefficient” would significantly influence the result. However, the upper constraint to insure adequate time for fully developed dispersion is still in place. Because of the upper restriction, a large Péclet number will require a very large aspect ratio in order for the dispersion to fully develop.

1.3 The dispersive process studied in this work

Most porous media does not contain straight channels, but rather channels which change in both direction and dimension. This irregular geometry can have significant effects on the structure of the velocity field as the flowrate increases and the viscous forces no longer dominate the inertial forces. The effect of axial curvature on the flowfield and related dispersion has been studied but will not be included

in this work. However, many processes, both natural and designed, involve flow through pores with highly variable cross-section [Batra et al., 1970]. Constrictions have been shown to significantly influence the pore-scale velocity field. For example, inertial flow through a constriction induces eddy formation on the lee side of the constriction [Weaver and Ultman, 1980].

The formation of eddies increases the complexity of the pore-scale velocity field which, in turn, has a significant effect on mass transfer. The fluid contained within these steady-state eddies experiences a significantly longer residence time than the inertial flow through the core of the tube [Turner, 1958]. As a result, molecular diffusion is the dominant mass transfer mechanism into and out of the eddies. Characterization of the eddies for averaging purposes is difficult as the size and stability of the eddies depend on the local flowrate as well as the local geometry.

In order to study the effect of these eddies on the dispersion, a model geometry must be selected which allows for a clear observation of the change in the macroscale behavior of the system when these eddies develop. Previous work [Hoagland and Prud'homme, 1985] has shown that sinusoidal tube is the simplest geometry with a periodically variable cross-section. While it is true that other functions (step functions, piece-wise function, etc.) also include periodic constrictions/expansions, this selection offers mathematical simplicity from both analytical and numerical perspectives. Sharp discontinuities that would occur in many of the piecewise options can generate flow instabilities. Sharp edges also require extensive refinement of numerical discretization.

The purpose of this study is to examine the dispersion of a solute within fluid

flowing through a sinusoidal tube. Numerical results are computed for a range of Reynolds numbers, from non-inertial creeping flow to inertia-dominated, steady laminar flow. Unsteady laminar flow is left for future studies. The solution is compared with a source-sink model commonly used to describe mass transport in porous media. The purpose of these comparisons is to examine the influence of a distribution of fluid residence time on macroscale dispersion.

Chapter 2 – Literature Review

2.1 Model Problems: Straight tubes

Given the difficulty in quantifying the microscale properties of real porous media, model geometries are often used to examine the influence of particular parameters. In 1953 Sir Geoffrey Taylor [Taylor, 1953] published a thorough analysis of advection-diffusion within a capillary tube. He generated two analytical solutions, one based on advection alone, and one based on the combined effect of advection and diffusion. The assumption was made that radial diffusion occurred quickly compared to the bulk flow of the fluid, and variance in concentration along the radial coordinate was neglected. Taylor then performed an experiment physically measuring the dispersion of potassium permanganate by colorimetry, and the results matched very well with the analytical solution for combined advection-diffusion. From the analytical solution, Taylor predicts that the dispersion coefficient should be

$$D = a^2U^2/48D_m \quad (2.1)$$

Taylor went on to validate the above solution for the following conditions [Taylor, 1954].

$$4L/a \gg aU/D_m \gg 6.9 \quad (2.2)$$

Rutherford Aris [Aris, 1959b] subsequently published an analytical solution to the advection-diffusion equation for a tube using the method of moments. His work resulted in the inclusion of the pure molecular diffusion coefficient in the definition of the dispersion coefficient, which was presented as

$$D_{eff} = D_m + a^2U^2/48D_m \quad (2.3)$$

This definition eliminates Taylor's lower constraint, which insured that the Péclet number (aU/D_m) was large enough to overshadow the effect of molecular diffusion, so that only the “apparent diffusion coefficient” would significantly influence the result. However, the upper constraint to insure adequate time for fully developed dispersion is still in place. Obviously, a large Péclet number will result in a very large aspect ratio (L/a) for the tube.

A similar asymptotic solution was developed for short times by Vrentas and Vrentas [Vrentas and Vrentas, 2000]. It was shown that at very early times, when axial diffusion overshadows axial convection, the solution is influenced more strongly by the diffusive term than the advective term even at large Péclet numbers. As time increases, the solution evolves to be much closer to the pure convective solution. Then as time increases further, the axial concentration distribution becomes asymmetric. If the Péclet number is very low then the concentration distribution closely resembles that of pure diffusion, even at the maximum allowable time for the asymptotic solution.

2.2 Taylor Dispersion: Early Time Solutions

Given that many physical systems do not reach the asymptotic solution, much work has been done on the time dependence of the dispersion coefficient at early times. Lighthill [Lighthill, 1956] published a solution for the concentration within a tube at very early times, but clearly pointed out the time gap between his analysis and Taylor's in which both theories incorrectly predict observed results. The solution is restricted to large Péclet numbers because axial diffusion is neglected. Furthermore it is only valid for portions of the solute which have not yet had any interaction with the tube walls, thereby restricting the description to the leading edge of the solute cloud.

Building on the work of Lighthill, and previous work by W.N. Gill [Gill, 1966] regarding dispersion within a time-dependent velocity field, Gill and Sankarasubramanian [Gill and Sankarasubramanian, 1970] produced a complete analytical solution for the advection-diffusion equation with time dependent dispersion coefficients via series expansion. The solution is plotted along with the Taylor solution and a pure advection solution for comparison. The distribution of the concentration along the axial coordinate at early times shows the disagreement between the time dependent case and the Taylor case. Several plots of concentration at a fixed point with respect to time show that as the distance between the initial pulse of solute and the monitoring point increases, the variance between the time-dependent curve and the Taylor curve decreases and eventually matches very well. This solution was later extended to include non-uniform initial solute distributions

[Gill, 1971]

Chatwin [Chatwin, 1970] developed an early time solution for the concentration distribution of laminar dispersion within a straight tube. By including axial diffusion in the development, Chatwin's solution contrasts with Lighthill's in that the initial distribution is asymmetrical, meaning it can account for fluid in contact with tube walls.

The flow in a majority of the straight tube problems is unidirectional. Barton [Barton, 1978] extended the theory to three dimensional flows to examine the early dispersion of a solute cloud. The solution shows that the early diffusion is predominantly isotropic but at late times only radial diffusion contributes significantly. However, the solution is only valid for times shorter than the time required to diffuse across domain and will not apply to flows with curvilinear streamlines.

In 1988, Vrentas and Vrentas [Vrentas and Vrentas, 1988] developed a perturbation solution for dispersion in laminar flow in a tube. At low Péclet numbers the solution is valid for both long and short times, and results are presented showing the transformation of the spatial solution with time. At early times, the solution closely resembles the pure diffusion solution, indicating that convection is less influential at very early times. This is because high concentration gradients drive a higher rate of diffusion and the convective term has a smaller effect. However, once the solute cloud has dissipated significantly, the perturbation solution more closely resembles the case of pure convection as would be expected.

Ekambara and Joshi [Ekambara and Joshi, 2004] developed a numerical solution for axial mixing of a slug of solute in laminar pipe flow. The generalized model

is shown to accommodate many special cases and reduces to the Taylor solution and also the asymptotic solution of Vrentas and Vrentas. The solution is valid at short and long times and a wide range of Péclet numbers.

2.3 Model problems: More complex geometries

In an effort to analyze a model geometry which incorporates some of the more complex geometric attributes common to, for example, porous media, examination of channels with varying cross-section has been studied under various conditions. Turner [Turner, 1958] examined a channel with rectangular pockets along the boundary. The fluid in these pockets, while not stagnant or immobile, experiences a substantially longer residence time than that of the flow along the axis of the channel. It was shown that diffusion is the dominant mass transfer mechanism within these pockets. A second model for multiple tubes of different lengths and diameters presents a theory for dispersion under the condition that the flow experiences a variety of residence times depending on the local channel within the medium. Aris [Aris, 1959a] subsequently provided a formulation for the Taylor dispersion coefficient based on the pocket model.

Peterson [Peterson, 1958] studied diffusion through pores of varying cross-section. In this work it was postulated that the converging-diverging nature of individual pores was inhibiting diffusion. This inhibition was previously assumed to be the result of tortuosity. These results are supported by Michaels. Michaels [Michaels, 1959] went on to point out that without detailed knowledge of the com-

plex geometry of most porous media, and concludes that pursuit of irregular pore models is unlikely to shed light on the dispersion mechanisms in actual porous media.

As a result of the converging-diverging geometry, the structure of the flow-field becomes very interesting as the inertial forces become significant to the flow. Payatakes et. al. [Payatakes et al., 1973] demonstrated via direct numerical simulation that steady-state eddies form in the diverging portions of the channel.

Weaver and Ultmann [Ultman and Weaver, 1979] examined by experiment the axial dispersion of gases passing through three constrictions of different geometry. They concluded that if the Reynolds number was large enough to produce flow separation below the constriction, but small enough for the flow to remain laminar, then dispersion increased significantly. However, once the Reynolds number reached a critical value and the jet produced by the constriction became turbulent, dispersion would decrease as the solute traveled with the bulk flow of the fluid. The increase in dispersion below the critical Reynolds number is due to the stalled fluid in the eddy downstream from the constriction and is proportional to the volume of the eddy.

Noting that a sinusoidal tube was the simplest geometry that included the converging-diverging nature of real porous media, Hoagland and Prud'homme [Hoagland and Prud'homme, 1985] conducted a numerical solution to a method of moments analysis of advection-diffusion in this geometry. The solution is valid for long times and low Péclet numbers. As the amplitude of the sine function approaches zero, the dispersion coefficient approaches the Taylor solution. The

dispersion coefficient increases with increasing amplitude. Inertial flow which produces eddies was not examined.

Many other model geometries have been utilized to examine porous media. Koo [Koo, 2006] studied dispersion in laminar flow past arrays of cylinders. Parks et. al. [Parks and Romero, 2006] studied dispersion in tubes with rectangular cross-section which provides insight into flows which are not axisymmetric. Kirchner and Hasselbrink [Kirchner and Hasselbrink Jr., 2005] examined electrokinetically driven transport through a variety of post arrays and wavy tubes. Detobel et. al. [Detobel et al., 2009] have studied the effect of dispersion in highly ordered silica monoliths with a focus on chromatographic applications. Dispersion within a bed of randomly packed spheres was examined via CFD by Jafari et. al. [Jafari et al., 2008].

Hlushkou and Tallarek [Hlushkou and Tallarek, 2006] provide a thorough review of the transition of flow within packed beds. It is noted that within these geometries the onset of turbulence is not sudden. Rather, the contribution of inertial forces gradually increases with the Reynolds number resulting in an intermediate viscous inertial regime. Within this viscous inertial flow, stationary eddies that are separate from the bulk inertial flow down the axis of the pore form on the lee side of the packing particles.

Cardenas [Cardenas, 2008] has conducted a thorough finite-element analysis of a single pore comprised of cubic-packed spheres and ellipsoids for the purpose of determining the effect of vortex formation on dispersion. The resulting breakthrough curve tails were shown to follow a power-law residence time distribution.

The power-law tailing is driven by the difference in local Péclet numbers between the vortices and the bulk flow. Cardenas [Cardenas, 2009] went on to show that as the solute passes through periodic unit cells, the power-law distribution gradually transforms into an exponential distribution.

2.4 Models for dispersion

A complete mathematical formulation for dispersion in spatially-periodic porous media based on Brownian motion theory was presented by Brenner [Brenner, 1980]. The thorough mathematical treatment provides a great deal of insight into the pore-scale behavior. It is clearly shown how the multi-directional velocity field contributes to dispersion. When the theory is applied to a straight tube, the solution reduced to the Taylor-Aris solution. However, the formulation is in terms of the local velocity vector. This requires complete resolution of the pore-scale velocity field in order for the solution to be applied to a specific problem.

Many researchers have applied Brenner's generalized theory to a specific problem. Chrysikopoulos et. al. [Chrysikopoulos et al., 1992] computed the mean velocity vector and dispersion dyadic for three-dimensional porous medium in which the retardation factor and the distribution coefficient are spatially-periodic. The distribution coefficient describes the rate of mass transfer from an immobile phase into the mobile phase. Both local equilibrium and first-order mass transfer models were examined. Solution was limited to unidirectional flow.

In order to accurately predict the macroscale dispersion, a clear link must be

established with the microscale properties which ultimately control the behavior of the system. In a later publication, Brenner [Brenner, 1990] detailed the relationship between the microscale and macroscale behavior of several generalized dispersion problems. This work demonstrates the variety of possible applications for accurate predictions of macroscale dispersion. It is pointed out that in general, the microscale behavior is only of interest due to the effect on macroscale behavior.

It is desirable to determine how the formation of eddies will influence dispersion within a porous medium. The suitability of first-order diffusion models to describe mass transfer in and out of eddies was examined by Griffioen [Griffioen, 1998]. It was found that a first order model does not hold for short periods of time.

Haggerty and Gorelick [Haggerty and Gorelick, 1995] presented a development of modeling diffusion via multiple-rate mass transfer. The diffusion process is assumed to be a distribution of first-order mass transfer models. Benchmark problems show that the method reduces to known solutions under idealized conditions.

The multi-rate model was expanded to describe mass transfer in a mobile-immobile system with advection-diffusion in the mobile domain and diffusive mass transfer in the immobile domain [Haggerty and Sean A. McKenna, 2000]. The transfer from the immobile domain to the mobile domain is represented with a source-sink term, developed in the paper for several model geometries as well as several distributions of first-order mass transfer coefficients.

Chapter 3 – Numerical Simulation

3.1 Geometry and Discretization

The numerical simulation was performed using the commercial finite-volume code STAR-CD. The computational domain was constructed in SolidWorks. A sine wave with a period of 2 units and an amplitude of 0.25 units was translated 0.5 units from the origin and then revolved 360 degrees about the origin. The initial length of the computational domain was 20 periods. A representative segment of sinusoidal tube is shown in Figure 3.1. This geometry was saved as a parasolid file and loaded into STAR-ccm+ for discretization, commonly referred to as “meshing.” The segment was meshed using the proprietary “Trim” mesh with prism layer option. The trim mesh is basically a structured cubic mesh. The prism layer is an unstructured mesh along the walls containing refined unstructured control

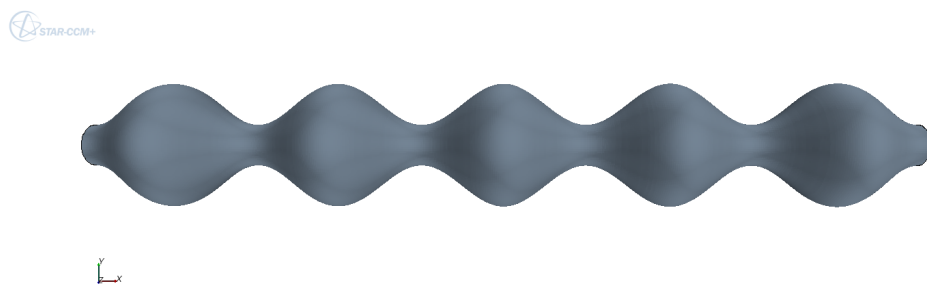


Figure 3.1: A segment of sinusoidal tube

volumes. The structured cubic mesh is preferable from a computational standpoint, as all control volume faces are parallel resulting in purely orthogonal flux. However, fitting a structured grid into an irregular geometry can be difficult. The prism layer of unstructured control volumes provides a smooth transition between the curvy surface of the tube and the cubic nature of the inner computation grid. Furthermore, by resolving the prism layer more than the bulk control volumes, the near-wall velocity gradients may be captured with more detail, thereby accurately including the wall-effects in the simulation. The resulting section was loaded into Pro-STAR, copied, translated, and merged iteratively to construct a computational domain 320 periods in length, containing 66.8 million control volumes. This mesh was scaled to be consistent with other pore-scale literature, and the final tube diameter at the widest part was 1.5 mm.

3.2 Simulation Conditions

The fluid properties were chosen to be consistent with liquid water. Both the inlet and outlet were defined with constant-pressure boundary conditions. While it is true that in inertial flow the pressure might not be radially uniform, the effect does not propagate far into the domain and will be neglected for the purpose of this study. The wall of the tube was defined using a no-slip boundary condition. Monitoring boundaries were placed perpendicular to the flow every 50 periods.

The governing partial-differential equations must be decomposed into a system of linear algebraic equations describing each control volume. A proprietary dis-

cretization scheme was implemented. The monotonic advection and reconstruction scheme (MARS) is a multi-dimensional second-order accurate differencing scheme that operates in two steps as described in the STAR-CD Methodology. First, the distribution of the property within a control volume is computed by interpolation from the surrounding control volumes using monotone gradients. By forcing the gradients to be monotone, the scheme is total variation diminishing, meaning the change in solution will never be greater in a subsequent iteration. The reconstructed cell properties are then used to compute the face fluxes using a monotone and bounded advection scheme.

Once the governing equations have been discretized, the resulting system of linear algebraic equations must be solved. For the steady-state flowfield solution this is accomplished using the SIMPLE algorithm in conjunction with an algebraic multi-grid solver. The SIMPLE algorithm is an implicit pressure correction method designed to enable fast, steady-state solutions to the Navier-Stokes equations by using a “pressure correction” rather than the coupled pressure to iterate through the implicit solution scheme. First the pressure and velocity gradients are computed using an initial guess or the results from a previous iteration. Next, the momentum equation is solved for an “uncorrected” velocity field and “uncorrected” mass fluxes at the cell faces. The pressure correction equation is then solved for each cell. However, due to the coupling of pressure and velocity, the pressure correction equation contains a velocity correction. This velocity correction is neglected in the SIMPLE algorithm. Finally, the velocity field and mass fluxes are corrected. The corrected pressure and velocity fields are then the basis

for computing the gradients for the next iteration. The residual tolerance was set at 10^{-8} for all steady-state flow variables.

Once the flowfield was determined the time-dependent transport equation was solved. The solute was assumed to be passive with respect to influencing fluid properties. The MARS discretization scheme was used, but this time in conjunction with the PISO algorithm and the algebraic multi-grid solver. The PISO algorithm is a time-marching scheme and is very efficient for solving transient problems. In this method, the velocity correction is approximated rather than neglected. This approximation allows for a time-accurate solution and thus is preferable to SIMPLE for transient problems. The entire domain was given a uniform initial solute concentration.

Data collection for the convection-diffusion problem involved computing the area-average and flux-average of the solute concentration at every monitoring plane and the outlet. Furthermore, the instantaneous solution over every control volume was saved periodically throughout the simulation.

3.3 Grid Convergence

The spatial and temporal discretization have a significant influence on the accuracy of a numerical solution. According to Roache [roa, 1998], a systematic grid convergence study is the most direct method for determining the influence of discretization on the final solution accuracy. A grid convergence study typically involves solving the desired equations over several domains of identical size but

increasingly refined discretization. Results of the solution are compared, and the solution is said to be “grid independent” when a doubling of computational elements results in a change in solution that is below a desired amount. The spatial discretization was computed by monitoring the total mass flux through the domain rather than picking a single point in order to examine a macroscale view of the grid convergence. For these studies, the grid was considered refined when the mass flux changed by less than 1% when the number of computational elements was increased by a factor of 2. The temporal grid-dependence was computed by taking the average difference between break-through curves between time-steps which differed by a factor of 2 for an inertial flowrate.

Chapter 4 – Results

4.1 Definitions

The Reynold's number was defined as

$$Re = \frac{\rho U a}{\mu} \quad (4.1)$$

where ρ is the fluid density, U is the average velocity, a is the radius at the widest part of the tube, and μ is the dynamic viscosity. The radius a was chosen because it represented the length scale for diffusion from the immobile region to the mobile region. The average velocity U is defined as the length of the tube divided by the superficial residence time or

$$U = \frac{L}{\tau} \quad (4.2)$$

The superficial residence time is defined as the total pore volume divided by the volume flux of the fluid or

$$\tau = \frac{V}{Q} \quad (4.3)$$

4.2 Flow observations

Hlushkuo and Tallarek [Hlushkou and Tallarek, 2006] reported that as the flowrate in packed beds increases there is a continuous transition from laminar flow to

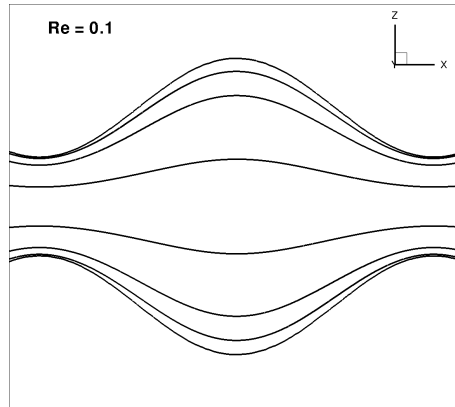


Figure 4.1: Non-inertial streamlines

inertial laminar flow before the onset of turbulence. Similar results were observed in this study, although the onset of turbulence was not reached. At the lowest flowrate, $Re = 0.01$, the flow is non inertial and laminar. The streamlines expand and contract with the tube as seen in Figure 4.1. Flow at $Re = 4.5$ (Figure 4.2) has significant inertial influence, although not enough to achieve streamline separation. However, the gradient in the diverging section is large, producing portions of fluid with obviously larger residence times despite the lack of flow separation. Note that in the diverging section, the streamlines are not completely aligned with the tube as at $Re = 0.1$. The inertial influence can be seen as the inflection point of the streamlines moves farther down the axis of the tube. Hlushkuo and Tallarek [Hlushkou and Tallarek, 2006] also reported that viscous-inertial flow is characterized by the development of an inertial core and steady-state, laminar eddies. This is observed clearly at $Re = 8.5$ shown in Figure 4.3. The velocity scale within the eddies is much lower than the velocity scale of the bulk flow. As

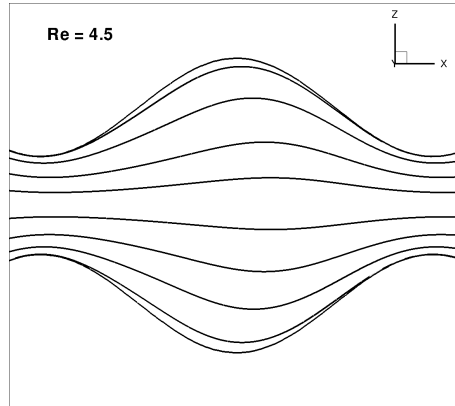


Figure 4.2: Streamlines at $Re = 4.5$

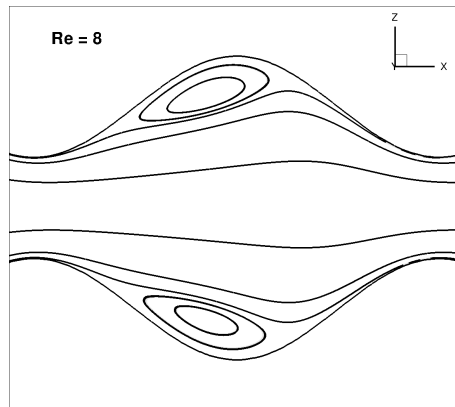


Figure 4.3: Streamlines at $Re = 8.5$.

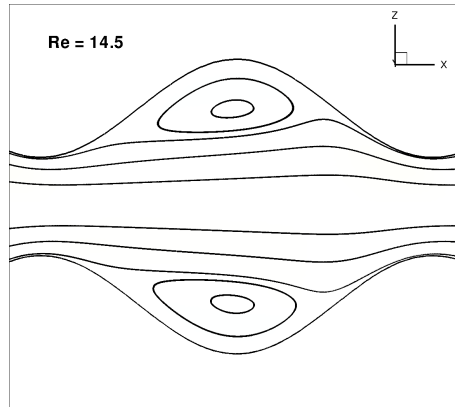


Figure 4.4: Inertial streamlines at $Re = 14.5$.

the flowrate increase further, the eddies increase in size and the axis of rotation moves toward the center of the diverging section, rather than forming more closely against the lee side of the constriction as at $Re = 8.5$. Streamlines for $Re = 14.5$ are shown in Figure 4.4.

4.3 Advection-Diffusion Observations: Early time

The influence of the velocity field on dispersion is significant. For non-inertial flow, the breakthrough curves (BTC) appear Gaussian. Although Hoagland and Prudhomme [Hoagland and Prud'homme, 1985] observed that the shape of the tube increases D_{eff} , the basic mechanism remains the same. However, for inertial flowrates the BTC's have a much different shape altogether. The early behavior is best observed in a plot on standard axes shown in Figure 4.5.

As the flowrate increases the BTC's “relax” successively, not only as a function

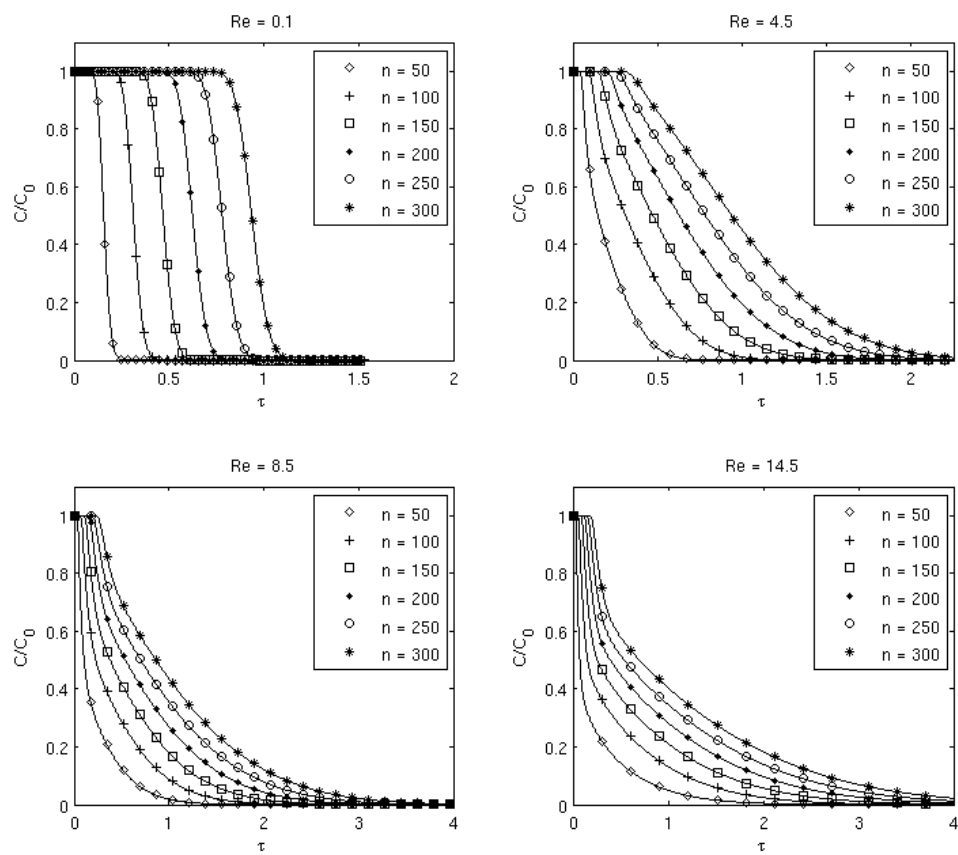


Figure 4.5: BTC for all flowrates plotted against residence time, τ

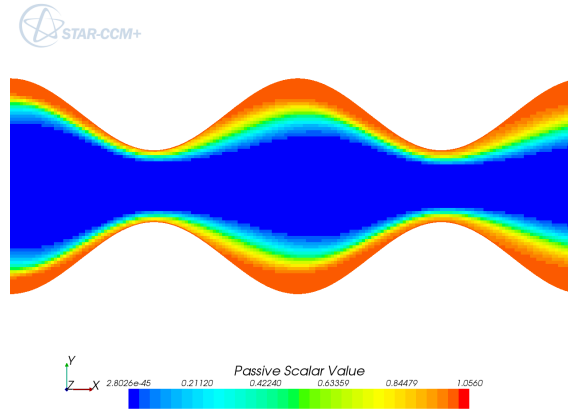


Figure 4.6: Concentration field for $Re = 4.5$ after the inertial core has initially cleared the central flow

of Re , but also as a function of axial distance down the tube. It should be noted that the eddies increase in size with Re . This not only results in a larger volume of fluid dominated by diffusion, but also in an increase in surface area over which the diffusion occurs. By examining the local concentration field it is observed that initially the inertial core clears the saturated fluid from the center of the tube leaving a large portion of saturated fluid in the eddies. Even at $Re = 4.5$, where no eddy formation was observed, the very slow moving fluid in the diverging sections is dominated by diffusion. Figure 4.6 shows the concentration field at $Re = 4.5$ after the inertial core has cleared the centerline of the tube.

As the flowrate increases further, eddy formation produces complex local mass transfer. The size of the slow-moving fluid increases, but the rotation of the eddies also results in diffusion from the outer layer. The center of the eddy retains its concentration longer than the fluid near the wall. This is clearly shown in Figure

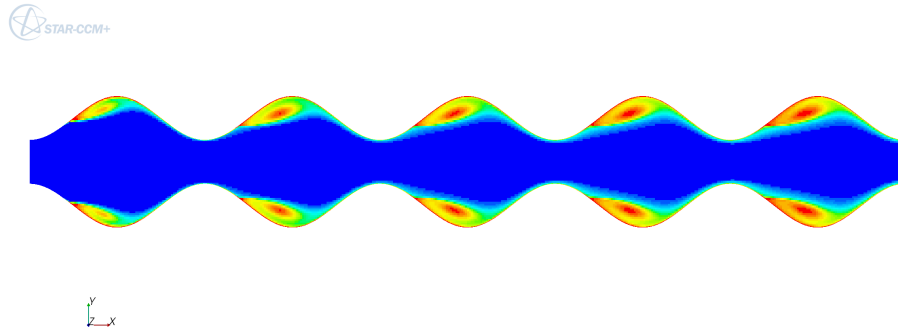


Figure 4.7: Local concentration field at $Re = 8$

4.7, the local concentration field for $Re = 8$ after sufficient time has passed for diffusion out of the eddies to create a local maximum at the center of rotation.

4.4 Advection-Diffusion Observations: Late times

The late time behavior of the BTC is best viewed on a plot with a logarithmic concentration scale, as shown in Figure 4.8. The non-inertial case ($Re = 0.1$) exhibits poor numerical stability at late times. This is due to roundoff error and was commonly experienced as the total concentration within the tube decreased below the resolution of the solver. Cardenas [Cardenas, 2009] studied the effect of three-dimensional vortices on transport and concluded that after ten periods the tailing could be described using a classic exponential model for the source-term in the 1-D advection-diffusion equation. The plots of the inertial cases at late times indicate an exponential tailing that is consistent with this observation.

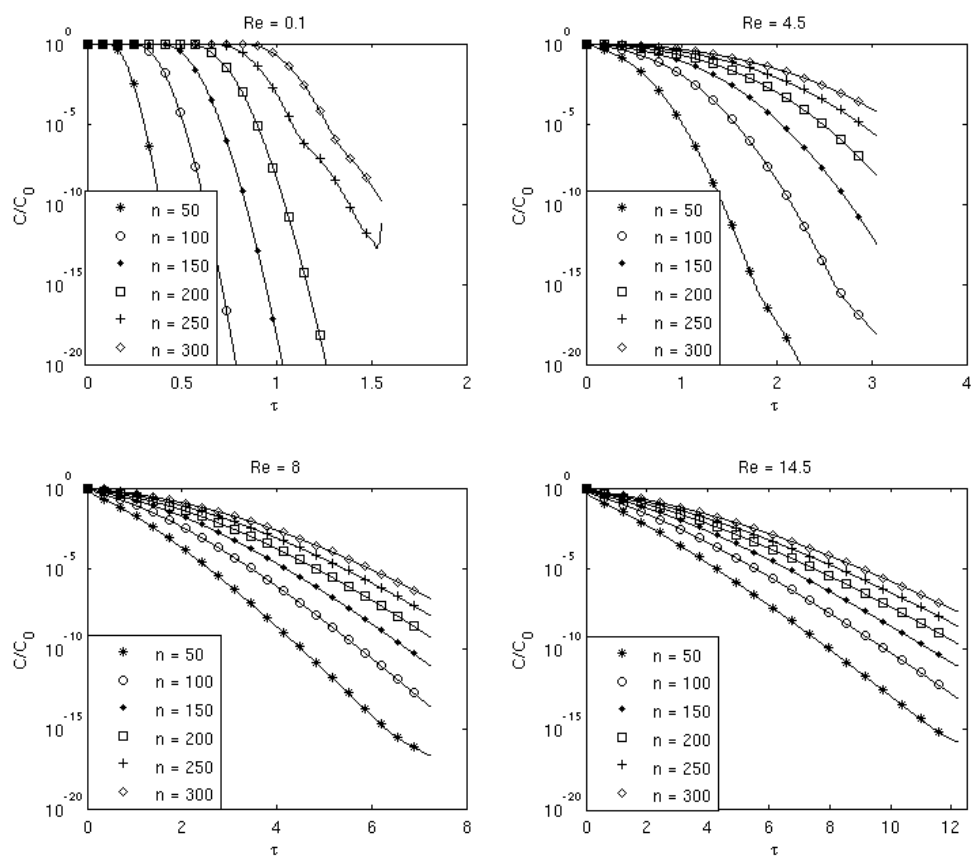


Figure 4.8: BTC's for all cases with logarithmic concentration scales

Chapter 5 – Analysis

5.1 General model for advection-dispersion with mass transfer

The 1-dimensional advection-diffusion equation previously discussed accounts for the pore-scale velocity gradients within the effective dispersion coefficient so that the solution accurately describes the macroscale mass transfer. However, due to the eddies in the diverging section, local velocity gradients are no longer the only physical process influencing the dispersion. It has already been shown that diffusion is the dominant mass transfer mechanism within the eddies, and that the fluid inside the eddies experiences a significantly longer residence time. If the fluid within the inertial core and the fluid within the eddies are segregated into separate, coupled domains, the 1-dimensional advection-dispersion equation could represent the inertial core if it was augmented with a source-sink term to account for diffusion into or out of the eddies. The 1-dimensional advection diffusion equation with mass transfer source-sink term describing the solute concentration in the inertial core is [Haggerty and Sean A. McKenna, 2000] :

$$\frac{\partial C}{\partial t} + \Gamma(x, t) = D_{eff} \frac{\partial^2 C}{\partial x^2} + U \frac{\partial C}{\partial x} \quad (5.1)$$

For this development a uniform initial condition is applied which is consistent with the numerical simulation.

$$C(x, t = 0) = C_0 \quad (5.2)$$

The boundary conditions are solute free flow at the inlet

$$C(x = 0, t) = 0 \quad (5.3)$$

and that the concentration far downstream will be equal to the initial condition at all time

$$c(x \rightarrow \infty, t) = C_0 \quad (5.4)$$

At late time dispersion is small compared to concentration

$$D_{eff} \frac{\partial C}{\partial x} \ll C, \quad (5.5)$$

and the time is much greater than the average advective time

$$t \gg t_{ad} \quad (5.6)$$

where t_{ad} is the average advective residence time, equal to L/U if velocity is constant in space. L is the point of observation. Furthermore, it is assumed that at late times, concentration does not change quickly with time and that $\Gamma(x, t)$ is the main source of change in C , or

$$\frac{\partial C}{\partial t} \ll \Gamma(x, t) \quad (5.7)$$

Applying eqns. 5.5 and 5.7 to 5.1, the concentration in the inertial core may be expressed as

$$-U \frac{\partial C}{\partial x} = \Gamma(x, t) \quad (5.8)$$

A simple integration provides an expression for C at L

$$C(x = L, t) = - \int_0^L \frac{1}{U} \Gamma(x, t) dx \quad (5.9)$$

If the parameters that make up $\Gamma(x, t)$ are spatially uniform then the concentration at late time is expressed as

$$C(x = L, t) = -t_{ad} \Gamma(t) \quad (5.10)$$

5.2 Development of the source-sink term, $\Gamma(t)$

A first-principles development of the source-sink term is non-trivial. In the case of a sinusoidal tube with eddies, the mass transfer is dependent on the size and rotational speed of the eddies as well as the concentration gradient within the eddies and the concentration gradient between the outer layer of the eddies and the inertial core. Fortunately, there has been a significant amount of research into quantifying the source-sink term for porous media with mass transport from an immobile, diffusion-dominated phase to a mobile advective-dispersive phase. The eddies that form in the flow within a sinusoidal tube are not immobile. However,

it is useful to determine if the influence of eddies on mass-transfer is similar to that of an immobile domain.

First, let us consider diffusive mass transport out of a control volume. The change in concentration over time can be expressed as the divergence of the diffusive flux of solute

$$\frac{\partial C_d}{\partial t} = \frac{\partial}{\partial y} \left(D_d \frac{\partial C_d}{\partial y} \right) \quad (5.11)$$

where C_d and D_d are the concentration and diffusivity in the diffusive domain and y is the distance away from the interface of the diffusive and advective-dispersive domains. For the simple case of two well-mixed fluids of differing concentration in contact through a partition, eqn. 5.11 reduces to [Haggerty and Gorelick, 1995]

$$\frac{dC_d}{dt} = \alpha(C - C_d) \quad (5.12)$$

The well-mixed assumption is not valid for many diffusion dominated cases, as concentration gradients will develop within the diffusive domain. However, it has been shown that a summation of various first-order rate coefficients can accurately represent the mass transport within a diffusion dominated fluid [Haggerty and Gorelick, 1995].

Let us return to Eqn. 5.11 and employ the following boundary conditions

$$C_d(x, y, t = 0) = 0 \quad (5.13)$$

$$C_d(x, y = 0, t) = C(x, t) \quad (5.14)$$

$$\frac{\partial C_d}{\partial y}(x, y = y_{max}, t) = 0 \quad (5.15)$$

where y_{max} is the point in the diffusive domain farthest from the interface with the advective-dispersive domain.

Let the solution for C_d for a constant C be $w(y, t)$. To find the solution for variable C , compute the convolution of w with $\frac{\partial C}{\partial t}$ [Carrera et al., 1998]

$$C_d(x, y, t) = \int_0^t \frac{\partial C}{\partial t}(x, t - \tau) w(y, \tau) d\tau \quad (5.16)$$

The convolution product is often written as “*”, so Eqn. 5.16 may be expressed as

$$C_d(x, y, t) = w(y, t) * \frac{\partial C}{\partial t} \quad (5.17)$$

Equation 5.17 completely describes the concentration in the diffusive zone. However, only the flux out of the diffusive zone influences the concentration profile in the advective-dispersive zone. The flux out of the diffusive zone is expressed by [Carrera et al., 1998]

$$\Gamma(x, t) = \alpha \left. \frac{\partial C_d}{\partial y} \right|_{y=0} \quad (5.18)$$

Substituting Eqn. 5.17 into 5.18 gives

$$\Gamma(x, t) = \alpha \frac{\partial}{\partial y} \left[w * \frac{\partial C}{\partial t} \right]_{y=0} \quad (5.19)$$

When the y -differential is distributed the expression becomes

$$\Gamma(x, t) = \alpha \left[\frac{\partial w}{\partial y} * \frac{\partial C}{\partial t} + w * \frac{\partial^2 C}{\partial y \partial t} \right]_{y=0} \quad (5.20)$$

C is undefined along y . As a result Eqn. 5.20 simplifies to

$$\Gamma(x, t) = \alpha \left[\frac{\partial w}{\partial y} * \frac{\partial C}{\partial t} \right]_{y=0} \quad (5.21)$$

Define

$$g(t) = \alpha \frac{\partial w}{\partial y}. \quad (5.22)$$

Now Eqn. 5.21 can be expressed as

$$\Gamma(t) = g(t) * \frac{\partial C}{\partial t} \quad (5.23)$$

where $g(t)$ is a memory function to be defined based on the spatial domain of C_d . The general form of the memory function is [Haggerty and Sean A. McKenna, 2000]

$$g(t) = \int_0^\infty \alpha b(\alpha) e^{-\alpha t} d\alpha \quad (5.24)$$

Here α is a rate coefficient and $b(\alpha)$ is a distribution function of first-order rate coefficients. In order for this model to accurately describe the mass transport process of interest, $b(\alpha)$ must be developed to accurately describe the local mass

transfer into the mobile domain. This will be discussed in §5.2.2.

5.2.1 Closure of $\Gamma(t)$

An approximation for C must be used in order to close the expression for $\Gamma(t)$ (Eqn. 5.23). The approximation should accurately describe both the initial condition and the late time value of C . Noting that at late times C approaches zero, the following approximation can easily describe a uniform initial condition and will be zero at late time [Haggerty and Sean A. McKenna, 2000].

$$C = m_0 \delta(t) \tag{5.25}$$

where m_0 is the zeroth moment of the initial condition. Employing the properties of convolution Eqn. 5.23 can be written as

$$\Gamma(t) = C * \frac{\partial g}{\partial t} + C g_0 - C_0 g \tag{5.26}$$

When the approximation for C is applied, it reduces to

$$\Gamma(t) = m_0 \frac{\partial g}{\partial t} - C_0 g \tag{5.27}$$

5.2.2 $b(\alpha)$ for a single-rate first order system

Let us first consider a single first-order mass transfer coefficient α_f . The density function is [Haggerty and Sean A. McKenna, 2000]

$$b(\alpha) = \beta_{tot}\delta(\alpha - \alpha_f) \quad (5.28)$$

where β_{tot} is ratio of mass in the immobile domain to that of the mobile domain at equilibrium. Substituting eqn. 5.28 into eqn. 5.24 and solving yields

$$g(t) = \alpha_f\beta_{tot}e^{-\alpha_f t} \quad (5.29)$$

Finally, the late-time concentration is given by substituting

$$C(x = L, t) = m_0 t_{ad} \beta_{tot} \alpha_f^2 e^{-\alpha_f t} \quad (5.30)$$

The form of this late-time solution is exponential. When plotted on semilog axes the solution should be a straight line with a slope of $-\alpha_f$.

In Figure 4.8, the late-time slope of the inertial cases is close to linear. That indicates that the first-order model might be appropriate to describe the late-time mass transport in the sinusoidal tube. Section 5.3 will describe the implementation of the solute-transport code STAMMT-L to estimate the single-rate parameters.

5.2.3 $b(\alpha)$ for a lognormal distribution of first-order rate coefficients

A lognormal distribution of first-order rate coefficients may be used to describe the local mass-transfer [Haggerty and Sean A. McKenna, 2000]. The density function is expressed as [Haggerty and Sean A. McKenna, 2000]

$$b(\alpha) = \sum_{j=1}^{\infty} \frac{8\beta_{tot}}{\sqrt{2\pi^5}(2j-1)^2\sigma\alpha} \cdot \exp\left[-\frac{[\ln(\frac{4\alpha}{(2j-1)^2\pi^2}) - \mu]^2}{2\sigma^2}\right] \quad (5.31)$$

where μ and σ are the mean and standard deviation of $\ln(D_a/a^2)$. The solution to this density function must be computed numerically.

5.3 STAMMT-L 3.0

A solute transport code, STAMMT-L [sta, 2009], was used to solve the mobile-immobile domain mass transfer problem presented in the previous section. The code uses a semi-analytical solution to solve for multiple immobile domains based on the multi-rate theory presented in Haggerty and Gorelick [Haggerty and Gorelick, 1995], and Haggerty et. al. [Haggerty and Sean A. McKenna, 2000]. The code was used to fit the data from the BTC of the monitoring boundary farthest from the inlet (0.6 m) using a single-rate model, and a lognormal multi-rate model. The code can fit up to 6 parameters, however only 4 were needed for the exponential model and 5 for the lognormal model. The parameters estimated using STAMMT-L were β_{tot} , the ratio of solute contained in the immobile phase to that of the mobile phase at equilibrium, α_L , the longitudinal dispersivity (not to be confused with the mass

transfer coefficients discussed in the previous section), vx , the pore-velocity for both models. For the single-rate model, α , the first-order mass transfer coefficient was determined. For the multi-rate model, μ and σ as defined in the previous section were determined. The residual calculations were performed in logarithmic space. This weights the tail of the BTC to more accurately fit the late-time data.

The results for the single-rate model are displayed in Table 5.1. The superficial average velocity, U , is provided for comparison.

Table 5.1: Fitted parameters from the single rate model

Re	U	vx	α_L	β_{tot}	$\ln(\alpha)$
0.1	$1.31x10^{-4}$	$1.4x10^{-4}$	$2.505x10^{-3}$	6.15	-2209
4.5	$6.2x10^{-3}$	$4.81x10^{-3}$	$2.33x10^{-2}$	$4.5x10^{-8}$	-27.4
8	$1.1x10^{-2}$	$1.5927x10^{-2}$	$3.603x10^{-2}$	1.46	448.7
14.5	$1.94x10^{-2}$	$2.9804x10^{-2}$	$5.0878x10^{-2}$	2.235	149.5

Looking at the parameters for $Re = 0.1$, the velocities match very well. Furthermore, the mass transfer coefficient, α is very close to zero. Virtually all of the solute is flushed from the tube with the advective fluid, so transfer from an immobile domain should not occur. Looking at $Re = 8$ and $Re = 14.5$, the fitted velocities are greater than the superficial velocities. This is also expected as Eqn. 4.2 does not account for the volume of the fluid in the eddies. The mass transfer coefficient is very large, but diffusion within the same fluid should occur on the order of the diffusivity of the fluid. The results for $Re = 4$ are not intuitively representative of the system. There is no physical reason why the fitted velocity should be less than the superficial velocity. Furthermore, the very small mass transfer

coefficient is not representative of the slow moving fluid which clearly influences the BTC. It seems that the single-rate model is fairly representative of the non-inertial case as well as the inertial cases with well defined separation. However, the unseparated flow with a large distribution of residence times seems to be too complex for the single-rate description.

The results from fitting the BTC with a lognormal multirate model are displayed in Table 5.2. The first 5 columns are the same as Table 5.1. The last two columns are the lognormal multi-rate parameters discussed in §5.2.3.

Table 5.2: Fitted parameters from the multi-rate model

Re	U	vx	α_L	β_{tot}	μ	σ
0.1	$1.31x10^{-4}$	$4.23x10^{-4}$	$2.15x10^{-3}$	2.05	-2955	∞
4.5	$6.2x10^{-3}$	$1.46x10^{-2}$	$2.31x10^{-2}$	2.02	-40.2	$3.49x10^{13}$
8	$1.1x10^{-2}$	$1.57x10^{-2}$	$3.6x10^{-2}$	1.43	210.5	0.0
14.5	$1.94x10^{-2}$	$2.05x10^{02}$	$5.07x10^{-2}$	1.22	103.3	$3.0x10^{-41}$

There is a similar correlation with the mass transfer coefficients, in that $Re = 4.5$ is greater than $Re = 0.1$, but $Re = 8$ is greater than $Re = 14.5$. The values for α_L are nearly identical to the values from the single rate model. However, for $Re = 0.1$ the fitted velocity is about 3 times as large, and the variance on the mass transfer coefficient is ∞ . The fitted velocity for $Re = 4$ is larger than the superficial velocity which is physically descriptive. However the variance on the mass transfer coefficient is very large. The velocity for the higher inertial cases are physically descriptive as well, and the variance of the mass transfer coefficients is nearly zero.

Chapter 6 – Conclusion

Advection-diffusion in a sinusoidal tube was modeled using the commercial finite-volume code STAR-CD. Both the early and late-time behavior was examined. The late-time data exhibited an exponential distribution as has been documented in the literature [Cardenas, 2009]. The results were compared to a 1-dimensional source-sink model. The source-sink term was determined using both a single-rate model and an exponential multi-rate model. It was found that both models can predict behavior of the inertial cases with fully formed eddies. However, the weak-inertial case, which did not have any flow separation but did have a large distribution of residence times within the fluid, was not handled well by either model. It seems that the separated flow acts, more or less, as an immobile region diffusing into the bulk flow. The weak-inertial case contains fluid which moves slower than the bulk flow, but is not completely separated and does not have the nearly-infinite residence time of the eddies in the high-inertial cases. This phenomenon is apparently difficult for the source-sink model to account for. Furthermore, while it was initially assumed that only separated eddies would significantly influence the dispersion, it was shown that even a large distribution of residence times within unseparated flow experienced a more complex dispersive process.

The results presented were non-dimensionalized and should scale well so long as the Reynolds number is maintained. However, the actual diameter of the tube

was chosen to be consistent with representative porous media. The diameter at the widest part of the tube was 1.5 mm. According to Hlushkou and Tallarek [Hlushkou and Tallarek, 2006] packed bed reactors are operated with bead sizes ranging from less than 1 mm up to several centimeters. A study examining mass transport within a hyporheic zone [Tonina and Buffington, 2007] indicates that particle size may vary from less than 1 mm up to greater than 25 mm. If the characteristic length is taken to be half the diameter of the particle, then an estimate of the flowrate required for inertial influences on dispersion can be obtained. Table 6.1 contains the minimum characteristic pore-velocity for a given particle size which would experience initially influenced dispersion.

Table 6.1: Minimum inertial pore velocities for a range of particle sizes

Diameter (mm)	v (m/s)
0.5	0.018
2	0.0045
5	0.0018
10	0.0009
25	0.00036
50	0.00018

Estimation of the volume of slow moving fluid relative to the volume of fast moving fluid is crucial to estimating the dispersion process in these complex geometries. Future work should be focused on quantifying the interaction of diffusion-dominated and advection-dominated fluids and how this interaction changes with Reynolds number.

Bibliography

- [roa, 1998] (1998). *Verification and Validation in Computation Science and Engineering*. Hermosa.
- [sta, 2009] (2009). *STAMMT-L Version 3.0 - User's Manual*.
- [Aris, 1959a] Aris, R. (1959a). “The longitudinal diffusion coefficient in flow through a tube with stagnant pockets”. *Chemical Engineering Science*, 11.
- [Aris, 1959b] Aris, R. (1959b). “On the dispersion of soluble matter flowing through a tube”. *Proceedings of the Royal Society of London*.
- [Barton, 1978] Barton, N. G. (1978). “The initial dispersion of soluble matter in three-dimensional flows”. *Journal of the Australian Mathematics Society*, 20.
- [Batra et al., 1970] Batra, V.; Fulford, G.; and F.A.L., D. (1970). “Laminar flow through periodically convergent-divergent tubes and channels”. *The Canadian Journal of Chemical Engineering*.
- [Brenner, 1980] Brenner, H. (1980). “Dispersion resulting from flow through spatially periodic porous media”. *Philosophical Transactions of the Royal Society of London*.
- [Brenner, 1990] Brenner, H. (1990). “Macrotransport Processes”. *Langmuir*, 6(12), pp. 1715–1724.
- [Cardenas, 2008] Cardenas, M. B. (2008). “Three-dimensional vortices in single pores and their effects on transport”. *Geophysical Research Letters*, 35.
- [Cardenas, 2009] Cardenas, M. B. (2009). “Direct simulation of pore level Fickian dispersion scale for transport through dense cubic packed spheres with vortices”. *Geochemistry Geophysics Geosystems*, 10(12).
- [Carrera et al., 1998] Carrera, J.; Sanchez-Vila, X.; Benet, I.; Medina, A.; Galarza, G.; and Guimera, J. (1998). “On matrix diffusion: formulations, solution methods and qualitative effects”. *Hydrology Journal*, 6.

- [Chatwin, 1970] Chatwin, P. (1970). “The approach to normality of the concentration distribution of a solute in a solvent flowing along a straight pipe”. *Journal of Fluid Mechanics*, 43.
- [Chrysikopoulos et al., 1992] Chrysikopoulos, C. V.; Kitanidis, P. K.; and Roberts, P. V. (1992). “Generalized Taylor-Aris moment analysis of the transport of sorbing solutes through porous media with spatially-periodic Retardation Factor”. *Transport in Porous Media*, 7.
- [Detobel et al., 2009] Detobel, F.; Gzil, P.; and Desmet, G. (2009). “Modeling the effect of species retention on the band broadening in perfectly ordered silica monolithic column mimics with variable external porosity and intra-skeleton diffusivity”. *Journal of Separation Science*, 32.
- [Ekambara and Joshi, 2004] Ekambara, K. and Joshi, J. (2004). “Axial mixing in laminar pipe flows”. *Chemical Engineering Science*, 59(18), pp. 3929–3944.
- [Gill, 1971] Gill, W. (1971). “Dispersion of a non-uniform slug in time-dependent flow”. *Proceedings of the Royal Society of London*, 322(1548).
- [Gill and Sankarasubramanian, 1970] Gill, W. and Sankarasubramanian, R. (1970). “Exact analysis of unsteady flow”. *Proceedings of the Royal Society of London*, 316(1526).
- [Gill, 1966] Gill, W. N. (1966). “Analysis of axial dispersion with time variable flow”. *Chemical Engineering Science*, 22.
- [Griffioen, 1998] Griffioen, J. (1998). “Suitability of the first-order mass transfer concept for describing cyclic diffusive mass transfer in stagnant zones”. *Journal of Contaminant Hydrology*, 34.
- [Haggerty and Gorelick, 1995] Haggerty, R. and Gorelick, S. M. (1995). “Multiple-rate mass transfer for modeling diffusion and surface reactions in media with pore-scale heterogeneity”. *Water Resources Research*, 31(10).
- [Haggerty and Sean A. McKenna, 2000] Haggerty, R. and Sean A. McKenna, L. M. (2000). “On the late-time behavior of tracer test breakthrough curves”. *Water Resources Research*, 36(12).
- [Hlushkou and Tallarek, 2006] Hlushkou, D. and Tallarek, U. (2006). “Transition from creeping via viscous-inertial to turbulent flow in fixed beds”. *Journal of Chromatography*, (1126).

- [Hoagland and Prud'homme, 1985] Hoagland, D. and Prud'homme, R. (1985). "Taylor-Aris dispersion arising from flow in a sinusoidal tube". *AICHE Journal*, 31(2), pp. 236–244.
- [Jafari et al., 2008] Jafari, P.; Zamankhan, A.; Mousavi, S.; and Pietarinen, K. (2008). "Modeling and CFD simulation of flow behavior and dispersivity through randomly packed bed reactors". *Chemical Engineering Journal*, 144.
- [Kirchner and Hasselbrink Jr., 2005] Kirchner, J. and Hasselbrink Jr., E. (2005). "Dispersion of a solute through post arrays and wavy-walled channels". *Analytical Chemistry*, 77(4).
- [Koo, 2006] Koo, S. (2006). "Taylor dispersion coefficients for laminar, longitudinal flow past arrays of circular tubes". *International Journal of Heat and Mass Transfer*, 50.
- [Lighthill, 1956] Lighthill, M. (1956). "Initial development of diffusion in Poiseuille flow". *IMA Journal of Applied Mathematics*.
- [Michaels, 1959] Michaels, A. S. (1959). "Diffusion in a pore of irregular cross-section - a simplified treatment". *AICHE Journal*, 5(2).
- [Parks and Romero, 2006] Parks, M. L. and Romero, L. A. (2006). "Taylor-Aris dispersion in high aspect ratio columns of nearly rectangular cross section". *Mathematical and Computer Modelling*, 46.
- [Payatakes et al., 1973] Payatakes, A. C.; Tien, C.; and Turian, R. M. (1973). "Part II. Numerical Solution of steady state incompressible flow through periodically constricted tubes". *AICHE Journal*, 19(1).
- [Peterson, 1958] Peterson, E. (1958). "Diffusion in a pore of varying cross-section". *AICHE Journal*, 4(3).
- [Taylor, 1953] Taylor, G. (1953). "Dispersion of soluble matter in a solvent flowing slowly through a tube". *Proceedings of the Royal Society of London*.
- [Taylor, 1954] Taylor, G. (1954). "Conditions under which dispersion of a solute in a stream of solvent can be used to measure molecular diffusion". *Proceedings of the Royal Society of London*.

- [Tonina and Buffington, 2007] Tonina, D. and Buffington, J. M. (2007). “Hyporheic exchange in gravel bed rivers with pool-riffle morphology: Laboratory experiments and three-dimensional modeling”. *Water Resources Research*, 43.
- [Turner, 1958] Turner, G. A. (1958). “The flow-structure in packed beds: A theoretical investigation utilizing frequency response”. *Chemical Engineering Science*, 7.
- [Ultman and Weaver, 1979] Ultman, J. and Weaver, D. (1979). “Concentration sampling methods in relation to the computation of a dispersion coefficient”. *Chemical Engineering Science*, 34(9), pp. 1170–1172.
- [Vrentas and Vrentas, 1988] Vrentas, J. and Vrentas, C. (1988). “Dispersion in laminar tube flow at low Peclet numbers or short times”. *AIChE Journal*, 34(9), pp. 1423–1430.
- [Vrentas and Vrentas, 2000] Vrentas, J. and Vrentas, C. (2000). “Asymptotic solutions for laminar dispersion in circular tubes”. *Chemical Engineering Science*, 55(4), pp. 849–855.
- [Weaver and Ultman, 1980] Weaver, D. and Ultman, J. (1980). “Axial dispersion through tube constrictions”. *AIChE JOURNAL*, 26(1), pp. 9–15.

